Geophys. J. Int. (2000) **141,** F1–F6

FAST-TRACK PAPER

Seismicity of the Sea of Marmara (Turkey) since 1500

N. N. Ambraseys[1] and J. A. Jackson[2]

[1] *Department of Civil Engineering, Imperial College, London,* SW7 2BU, *UK. E-mail: n.ambraseys@ic.ac.uk*
[2] *University of Cambridge, Department of Earth Sciences, Bullard Laboratories, Madingley Road, Cambridge,* CB3 OEZ, *UK. E-mail: jackson@esc.cam.ac.uk*

Accepted 2000 February 29. Received 2000 February 25; in original form 1999 November 22

SUMMARY

We use the earthquake history of the last 500 years to help evaluate the tectonic and hazard contexts of the 1999 earthquakes at Izmit and Düzce in western Turkey. The 20th century has been unusually active, but over the 500 year period the seismic moment release can account for the known right-lateral shear velocity across the Marmara region observed by GPS. Two areas of known late Quaternary faulting stand out as unusually quiet over this period: the northwest shore of the Sea of Marmara and the southern branch of the North Anatolian fault system between Bursa and Mudurnu.

Key words: active tectonics, earthquakes, seismic hazard, Turkey.

1 INTRODUCTION

This paper was prompted by the catastrophic earthquakes of 1999 August 17 and November 12 near Izmit and Düzce (Barka 1999; Toksöz *et al.* 1999), at the eastern end of the Marmara Sea in northwest Turkey, which raised several questions that must be addressed in any realistic assessment of the future seismic hazard to that populous area of Turkey. In particular: (1) is the 20th century seismic activity of the Marmara region, which has included five earthquakes of $M_s \geq 7$, representative of longer periods; (2) how is the long-term distribution of large earthquakes related to known late Quaternary faults; (3) how do the 1999 earthquakes compare with earlier historical earthquakes that damaged Istanbul; and (4) is it likely that, in the long term, seismic slip on faults accounts for all or most of the tectonic motion in the region, the rate of which is now well known from GPS measurements, or is aseismic creep significant? The object of this paper is to make available some historical data that can be used to investigate these questions.

2 TECTONICS

The active tectonics of northern Turkey is dominated by the right-lateral North Anatolian fault zone, running from Karliova in the east (41°E) to Istanbul (29°E) in the west. Over much of this distance the fault zone is a clearly defined morphological feature that in some ways resembles a plate boundary in that it is narrow, localized and separates the effectively rigid Black Sea and central Anatolia regions (e.g. McClusky *et al.* 2000). The zone has produced many large ($M_s > 7$) earthquakes with coseismic surface faulting and ruptured over most of its length this century in a sequence of large events between 1939 and 1999 (Ambraseys 1970; Barka 1996; Stein *et al.* 1997). Right-lateral strike-slip faulting continues west of Izmit (Fig. 1a) but becomes more distributed over several subparallel strands in the Sea of Marmara, NW Turkey and the northern Aegean (e.g. Barka & Kadinsky-Kade 1988; Taymaz *et al.* 1991). Seismic reflection surveys in the Sea of Marmara itself reveal many faults with large normal components (e.g. Smith *et al.* 1995; Okay *et al.* 1999; Parke *et al.* 2000), and earthquakes with normal-faulting mechanisms are seen around its margins (Fig. 1a). The Sea of Marmara was presumably formed by this component of crustal extension. GPS surveys demonstrate that the E–W shear across the region of Fig. 1 is about 23 ± 3 mm yr^{-1} (Straub *et al.* 1997; McClusky *et al.* 2000).

3 EVALUATION OF LONG-TERM SEISMICITY

3.1 Approach

For the 20th century we recalculated surface wave magnitudes uniformly from reported amplitude and period observations using the Prague formula. Using case histories and detailed discussions of individual earthquakes (mostly from Ambraseys 1988) we were then able to establish empirical relations between intensity distribution and M_s.

For the period 1500–1900 the historical record is good enough to use these empirical intensity–magnitude relations to estimate M_s for the larger earthquakes. For the 16th–18th

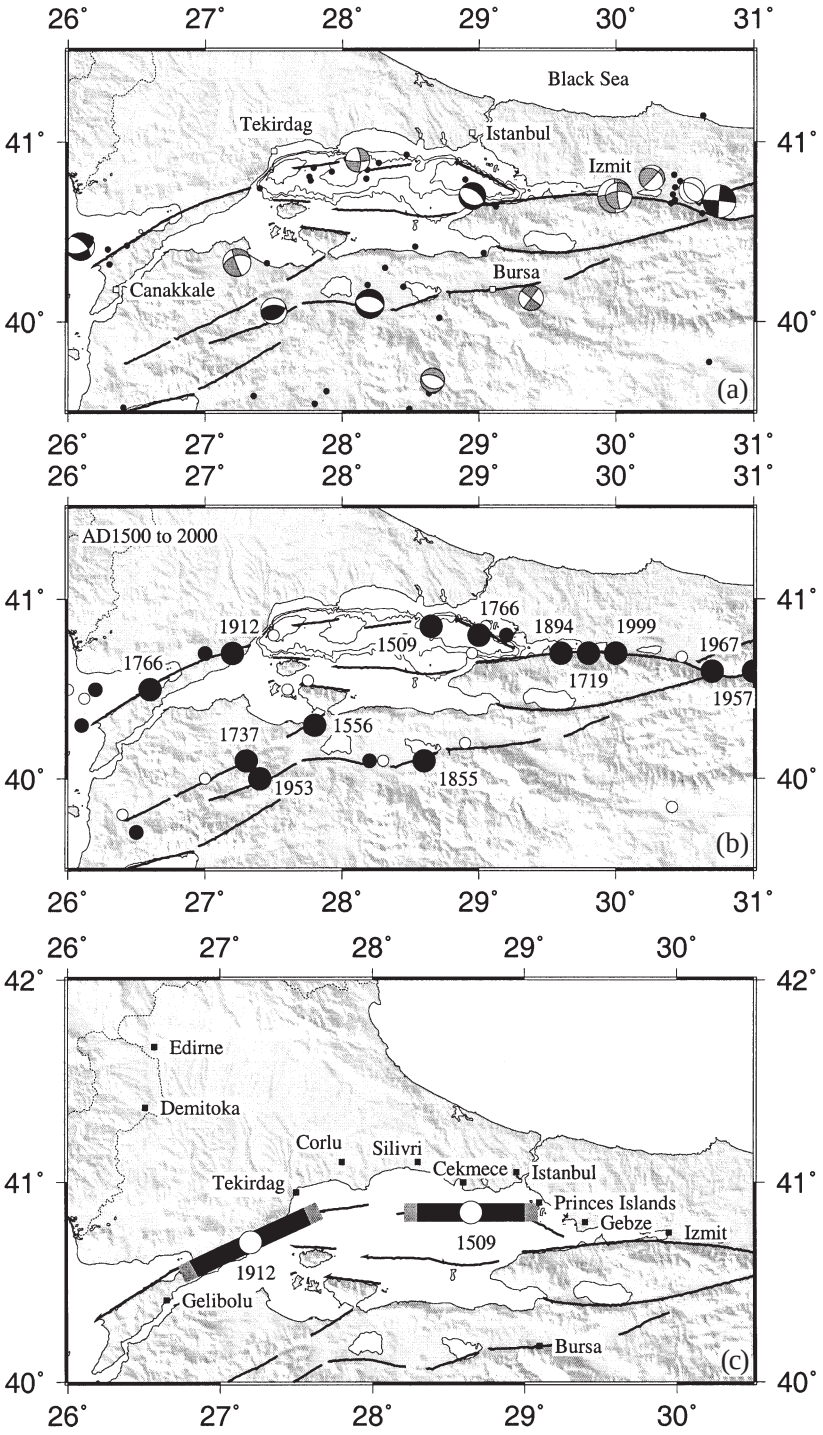

Figure 1. (a) Modern fault plane solutions and major active faults in the Sea of Marmara region. Faults are adapted from Barka & Kadinsky-Kade (1988) and Parke *et al.* (2000). Black focal mechanisms are from Taymaz *et al.* (1991), dark grey ones are Harvard CMT solutions, and the light grey one is a first-motion solution from McKenzie (1978). Black filled circles are epicentres between 1964 and 1995 from Engdahl *et al.* (1998). (b) Major earthquakes in the Marmara region from Table 1. Large black circles are events of $M_s \geq 7.0$, small black circles are those of $7.0 > M_s \geq 6.6$, and white circles are those of $6.6 > M_s \geq 6.0$. Only those with $M_s \geq 7.0$ are labelled with dates. Note that the locations of earthquakes before 1900 represent the approximate centres of the macroseismic regions; earthquakes of M_s 7.0–7.2 will have ruptured faults $\sim$40–60 km in length. (c) Location map for discussion of the 1509 September 10 and 1912 August 9 earthquakes. The black bars show the estimated rupture lengths for these earthquakes, based on eq. (3) and using a value for W of 15 km. The rupture length estimates increase to the shaded bars if we use $W = 10$ km.

centuries case histories are taken from Ambraseys & Finkel (1995) and unpublished sources. Detailed case histories for the 19th century, based on our own research, will be published elsewhere. We believe we have identified, and estimated magnitudes for, all earthquakes in the Marmara region with $M_s \geq 6.8$ since 1500, as well as many that are smaller (Table 1). The data for earthquakes prior to 1500 are patchy and not suitable for the same treatment.

Table 1. This table contains all the earthquakes between 1500 and 2000 AD with $M_s \geq 6.0$ of which we are aware. We believe it is complete (i.e. that none are missing) above $M_s \geq 6.8$ but incomplete below that threshold. Locations are the centres of the macroseismic regions and are known only to 0.1° (at best); some are given to greater accuracy only to distinguish them on the map in Fig. 1(b). Moments for earthquakes of $M_s \geq 6.8$ are given in units of 10^{19} N m. M_0^a is calculated from Ekström & Dziewonski's (1988) global M_s–M_0 relation; M_0^b is calculated from the new bilinear M_s–M_0 relation for the Middle East described in the text. M_0^{obs} is the observed moment calculated from long-period *P* and *SH* body waves for 1964 October 6 and 1967 July 22 (Taymaz *et al.* 1991) or from the Harvard CMT solution for 1999 August 17. L is the expected fault rupture length calculated using eq. (3) and a seismogenic thickness (*W*) of 10 km.

Year	Date	Time	Lat.	Long.	M_s	M_0^a	M_0^b	M_0^{obs}	L
1509	Sept. 10	2200	40.9	28.7	7.2	10.00	8.42		74
1556	May 10	2400	40.3	27.8	7.2	7.85	6.61		66
1719	May 25	1200	40.7	29.8	7.4	18.62	15.67		102
1737	Mar. 6	0730	40.1	27.3	7.0	4.37	3.67		49
1754	Sept. 2	0330	40.8	29.2	6.8	2.43	2.04		36
1766	May 22	0500	40.8	29.0	7.1	5.96	5.01		58
1766	Aug. 5	0530	40.5	26.6	7.4	14.62	12.31		90
1809	Feb. 7	0000	40.0	27.0	6.1				
1826	Feb. 8	2030	39.8	26.4	6.2				
1841	Oct. 6	0230	40.85	29.05	6.1				
1850	Apr. 19	2330	40.1	28.3	6.1				
1855	Feb. 28	0230	40.1	28.6	7.1	6.17	5.19		59
1855	Apr. 11	1940	40.2	28.9	6.3				
1859	Aug. 21	1130	40.3	26.1	6.8	2.10	1.78		34
1860	Aug. 22	1009	40.5	26.0	6.1				
1893	Feb. 9	1716	40.5	26.2	6.9	3.09	2.60		41
1894	July 10	1224	40.7	29.6	7.3	11.48	9.66		80
1912	Aug. 9	0128	40.7	27.2	7.3	12.74	10.72		‡84
1912	Aug. 10	0923	40.8	27.5	6.2				
1912	Sept. 13	2331	40.7	27.0	6.8	2.51	2.11		37
1935	Jan. 4	1441	40.50	27.60	6.4				
1935	Jan. 4	1620	40.55	27.75	6.3				
1943	June 20	1532	40.68	30.48	6.4				
1944	Oct. 6	0234	39.7	26.5	6.8	2.43	2.04		37
1953	Mar. 18	1906	40.0	27.4	7.1	5.37	4.52		‡55
1956	Feb. 20	2031	39.84	30.41	6.2				
1957	May 26	0633	40.6	31.0	7.2	7.85	6.61		‡66
1963	Sept. 18	1658	40.70	28.95	6.4				
1964	Oct. 6	1431	40.1	28.2	6.8	2.17	1.84	0.41	35
1967	July 22	1657	40.7	30.7	7.2	9.02	7.59	7.50	‡71
1975	Mar. 27	0515	40.45	26.12	6.5				
1983	July 5	1201	40.28	27.76	6.1				
1999	Aug. 17	0001	40.7	30.0	7.4	17.38	14.63	†21.00	‡98

† The USGS CMT solution gives a moment of 14.0 for this event.
‡ Observed lengths of surface ruptures were approximately 50 km (1912), 58 km (1953), 40 km (1957), 80 km (1967) and 120 km (1999); see Ambraseys & Jackson (1998) and Barka (1999).

3.2 Assessment of intensity

Since intensity distributions are used to estimate magnitude for the pre-1900 events, some remarks on the data are appropriate. During the period from 1500 to the early 1900s, the few large towns are the main sources of information, and the distribution of earthquakes discussed in historical sources is often closely related to the distribution of these urban centres. In the larger urban centres that are affected such as Istanbul, the damage is usually reported in greater detail and often with some exaggeration. Occasional mention is sometimes made of shaking in far-off places that turn out not to have been affected by the same earthquake, and these reports can also exaggerate the estimate of earthquake size.

Local houses in the plains were of mud-wall or adobe-brick construction covered with flat and heavy roofs, consisting of a rough boarding covered with tamped earth. In mountain villages houses were usually built with rubble-stone masonry laid in clay mortar in terraces, often with the roof of one house being the yard of the house above. In large villages and in towns the majority of houses, one to three storeys high, were built chiefly of wood, while stone-masonry construction was

used chiefly for public buildings, places of worship and forts. Better houses on the outskirts of towns and in a few large villages were often detached and surrounded by a garden and a high wall. Elsewhere houses were built close together in clusters, separated by narrow, winding alleys, and in some cases on sloping ground. In many cases it is practically impossible to determine how strong or light a shock would be necessary to cause damage or destruction. The same applies to secondary effects such as landslides, rockfalls and soil failure, all of which are of limited value in assessing intensity.

In addition, damage statistics are totally lacking and descriptions are brief and stereotyped. Maximum intensity appears to be effectively the same; that is, at intensity VIII MSK, all adobe and rubble-masonry houses are destroyed and any village or town would thus appear equally, but no more, devastated at so-called higher intensity. Higher intensities can only be assessed from the behaviour of timber-framed constructions with higher resistance.

As a consequence of these problems, any attempt to draw isoseismals of intensity greater than VI for these early earthquakes would be very subjective, and it is only for sites removed from the epicentral area and for which there is sufficient information that it is possible to assess intensities smaller than VIII. Conventional intensity scales are too subjective and quite misleading for these earlier events, especially in the higher range of the scale.

In our intensity assessment we used only low intensity ratings, taking into consideration that for large earthquakes ($M_s > 7$) with surface faulting, site distances must be measured from the earthquake source (probable fault) rather than from the epicentre, which for early or off-shore events is rarely known with any accuracy.

3.3 Magnitude assessment

The surface wave magnitude M_s of pre-1900 earthquakes was estimated from the intensity distribution using the equation

$$M_s = -1.54 + 0.65(I) + 0.0029(r) + 2.14\log(r) + 0.32p\,, \qquad (1)$$

where M_s is the uniformly recalculated surface wave magnitude, I ($<$ VIII) is the intensity at a site at a distance r (km) from the source, and p is 0 for mean values and 1 for 84 percentile. Eq. (1) was derived from 488 isoseismals of about 9000 intensity points associated with 123 shallow ($<$26 km) earthquakes in Greece and Western Turkey (Ambraseys 1992). Eq. (1) gives similar results to

$$M_s = +0.79 + 0.46(I) + 0.0018(r) + 1.56\log(r)\,, \qquad (2)$$

which was derived for shallow earthquakes in Greece (Papazachos 1992) for all intensities.

Our intensity estimates for historical earthquakes are accurate only to ± 0.5 intensity units at best, corresponding to an uncertainty in M_s, from eqs (1) and (2), of ± 0.3 magnitude units.

3.4 Moment estimates

We estimated seismic moments from surface wave magnitudes for all events of $M_s \geq 6.6$ in two ways. First we used the global M_s–M_0 relation of Ekström & Dziewonski (1988) based on 2341 M_s–M_0 pairs from the USGS Preliminary Determination of Epicentres (PDE) and Harvard CMT catalogues:

$$\log M_o = 19.24 + M_s \qquad \text{for } M_s < 5.3\,,$$
$$\log M_o = 30.20 - (92.45 - 11.40M_s)^{0.5} \qquad \text{for } 5.3 \leq M_s \leq 6.8\,,$$
$$\log M_o = 16.14 + 1.5M_s \qquad \text{for } M_s > 6.8\,,$$

where M_0 is in dyne cm. We also calculated a regional M_s– M_0 relation for the eastern Mediterranean and Middle East based on 609 M_s–M_0 pairs binned into units of 0.2 in M_s and 0.2 in $\log M_0$. We sought a bilinear relation with slope 1.0 at low M_s and slope 1.5 at high M_s (for which there is theoretical justification; see Ekström & Dziewonski 1988) and obtained

$$\log M_o = 19.083 + M_s \qquad \text{for } M_s \leq 6.03\,,$$
$$\log M_o = 16.065 + 1.5M_s \qquad \text{for } M_s > 6.03\,,$$

with M_0 in dyne cm. The regional relation yields smaller M_0 values for a given M_s, and it is not clear which is the better relation for earthquakes of $M_s > 7.0$ in this part of Turkey. There are only two recent earthquakes of $M_s > 7.0$ in this paper for which direct measurements of M_0 are possible (in 1967 and 1999; see Table 1), and for these it appears that the global relation yields M_0 values too high while the regional relation yields values closer to those observed.

4 RESULTS

4.1 Seismicity distribution in space and time

Fig. 1(b) and Table 1 show all the events in the period 1500–1999 for which our sources suggest a magnitude $M_s \geq 6.0$. We believe that the list in Table 1 is complete for earthquakes of $M_s \geq 6.8$, but not for smaller events. For earthquakes before 1900 the locations we give are the centres of the macroseismic regions and are necessarily approximate, bearing in mind that earthquakes of M_s 7.0–7.2 will have ruptured faults $\sim$40–80 km in length. A rough estimate of the probable fault rupture length (L) in each case can be obtained from

$$L^2 = \frac{M_0}{\mu W \alpha}\,, \qquad (3)$$

where M_0 is the seismic moment, μ is the rigidity ($\sim 3.0\times10^{10}$ N m^{-2}), W is the thickness of the seismogenic layer (probably 10–15 km) and α is the ratio of incremental slip to fault length, which is typically $\sim 5\times10^{-5}$ for intraplate earthquakes (Scholz *et al.* 1986). Estimated values of L are given in Table 1 for events of $M_s \geq 6.8$ assuming $W = 10$ km. Since L depends on the square root of M_0 and W, small changes in the values of M_0 and W do not have a big effect on estimates of L: changing W to 15 km reduces the values of L in Table 1 by a factor of 0.8.

4.2 The 20th century and Istanbul

It is immediately clear from Fig. 1(b) and Table 1 that the 20th century has been unusually active, with five earthquakes of $M_s \geq 7.0$ (or six if the M_w 7.1 Düzce earthquake of 1999 November 12, just east of the region we consider at 31.2°E, is included). Only the 18th century, with four events of $M_s \geq 7.0$ has had comparable activity. For two long periods of 163 years (1556–1719) and 89 years (1766–1855) there were no earthquakes above our completeness threshold of $M_s \geq 6.8$. This is

not due to a lack of data, as these periods are relatively well documented and provide information about many earthquakes below our threshold magnitude. During these periods of relative quiescence in the Marmara region, the North Anatolian fault system was much more active further east, producing several large earthquakes of $M_s \geq 7.0$.

The greatest damage in Istanbul was caused by the earthquakes of 1509, 1754 and 1766. These seem to have been in the magnitude range M_s 6.8–7.2, with their macroseismic effects clearly indicating a magnitude smaller than the largest events of 1719 (M_s 7.4), 1912 (M_s 7.3) and 1999 (M_s 7.4). The implication is that they ruptured relatively short faults of ~ 70 km length or less offshore, compared to the ruptures of > 100 km length that characterize the largest events onshore. This is consistent with the evidence from seismic reflection surveys in the Sea of Marmara, showing that faults are generally less continuous offshore than onshore (Parke *et al.* 2000).

4.3 Quiescence in the northwest Sea of Marmara

In the period between 1500 and 2000 we found no evidence for large ($M_s > 6.6$) earthquakes in the northwest and north-central part of the Sea of Marmara between the regions affected by the 1912 and 1509 earthquakes. This important conclusion depends critically on our interpretation of those two earthquakes.

Most of the damage in the 1509 September 10 earthquake was along a 100 km strip of the NE coast of the Sea of Marmara, between Silivri and Gebze (Fig. 1c), including Çekmece, Istanbul and the Princes Islands, where intensities were VII or greater. The shock caused panic at Çorlu and cracking of houses at Gelibolu. At Demitoka some repairs to the palace may have been required by the earthquake but there is no evidence of other damage, and only minor damage to a mosque and hospital is described at Edirne. To the east, the shock caused some damage in Izmit, but this was probably minor as no mention is made of any public buildings needing repairs. We could find no evidence of damage on the south coast of the Sea of Marmara, although there may have been minor effects at Bursa, where the public baths were repaired at this time. There are no direct reports from Tekirdag (Rodosto), but it is significant that Tekirdag and Demitoka contributed the largest number of masons to the reconstruction of Istanbul, suggesting that damage to those towns was slight. The 1509 earthquake excited widespread contemporary interest because of the great ruin it caused locally at Istanbul, rather than because of its large magnitude or because its destructive effects were widespread. Heavy damage was concentrated either side of Istanbul, and was confined to the NE part of the Sea of Marmara. Our estimated magnitude for this event suggests a fault length of about 60–70 km (Table 1, Fig. 1c), which would extend from near Silivri to the Princes Islands, which is consistent with the damage distribution.

The 1912 August 9 earthquake ruptured the Gelibolu peninsula (Ambraseys & Finkel 1987). Although the NE end of the surface faulting entered the Sea of Marmara, damage declined rapidly NE around the coast towards Tekirdag, suggesting that rupture did not extend far offshore. Severe destruction was limited to the peninsula itself and did not spread to the NW coast of the Sea of Marmara. Fig. 1(c) shows our expected fault length for this earthquake, centred in the middle of the region of maximum damage.

In Fig. 1(c) we have deliberately plotted the estimated ruptures for the 1912 and 1509 earthquakes as far east and west (respectively) as we think reasonable. Even if we use the higher values of estimated fault lengths obtained by taking $W = 10$ km, it seems extremely improbable that the 1912 and 1509 ruptures met or overlapped, a conclusion that is consistent with our estimates of the sizes and with the damage distributions in the two events. There is thus no evidence for significant rupture of the offshore region between Silivri and Tekirdag between 1500 and the present day, even though the right-lateral strike-slip motion must continue through this region, as demonstrated by the single small (M_w 5.3) CMT solution of 1988 April 24 (Fig. 1a). We conclude that the absence of large, damaging earthquakes along the northern shore of the Sea of Marmara is almost certainly real: the region has always been a major trade route and is well covered by contemporary accounts that reveal small events, but nothing substantial. Our preliminary research on the period prior to 1500 has also failed, so far, to reveal any substantial earthquakes along the northern shore of the Sea of Marmara. Although Toksöz *et al.* (1999) placed the epicentral region of the 1766 May 22 earthquake offshore between Silivri and Çekmece (see our Fig. 1c and their Fig. 6), this is not correct: damage was concentrated east rather than west of Istanbul and extended east of the regions affected in 1509 (Ambraseys & Finkel 1995).

4.4 Quiescence east of Bursa

A second obvious anomaly is the southern branch of the strike-slip system between the 1967 epicentre at Mudurnu and Bursa where, in spite of fault morphology suggesting late Quaternary activity (e.g. Barka 1996), there have been no substantial earthquakes in the last 500 years. GPS measurements also suggest that this southern branch of the fault system is less active than that to the north, through Izmit (Straub *et al.* 1997). However, historical sources reveal high seismic activity on the fault system prior to 1500 between Bursa and Mudurnu, including a large earthquake in 32 AD near Iznik (Nicea).

4.5 Seismic slip rates

We summed the scalar seismic moments of the earthquakes in Table 1 to obtain estimates of the right-lateral shear velocity through the region, using a seismogenic thickness of 15 km and assuming a value for the rigidity of $\mu = 3.0 \times 10^{10}$ N m^{-2}. We assume that each event of $M_s \geq 6.8$ contributes to this motion. It is possible that some of the earlier smaller events may have had normal faulting mechanisms, but the modern normal faulting events are all of $M_s < 6.3$, in keeping with the generally short normal fault segments, so we do not think the assumption that the events of $M_s \geq 6.8$ are all strike slip is an important source of error.

The earthquakes of $M_s \geq 6.8$ account for 15.3 mm yr^{-1} of right-lateral motion using the global M_s–M_0 relation and 12.9 mm yr^{-1} using the regional relation (Table 2). These estimates increase to 26.0 and 21.9 mm yr^{-1} allowing for earthquakes of $M_s < 6.8$, which increase the total moment by a factor of 1.7 (e.g. Ambraseys & Sarma 1999), and increase still further to 39 and 33 mm yr^{-1} if the seismogenic thickness is reduced to 10 km. The velocity estimated from GPS measurements is 22 ± 3 mm yr^{-1} (Straub *et al.* 1997).

Table 2. Estimated right-lateral shear velocities in the Marmara region. Lines 1 and 2 are estimated from the summed moments of earthquakes since 1500. Line 1 is based on the global M_s–M_0 relation of Ekström & Dziewonski (1988). Line 2 is based on the bilinear regional relation discussed in the text. V ($M_s \geq 6.8$) is the velocity accounted for by earthquakes of $M_s \geq 6.8$. V (total) includes the estimated contribution of earthquakes with $M_s < 6.8$. Line 3 is the GPS estimate from Straub *et al.* (1997).

	Source	V ($M_s \geq 6.8$) mm yr^{-1}	V (total) mm yr^{-1}
1	global M_s–M_0 relation	15.3	26.0
2	bilinear regional M_s–M_0 relation	12.9	21.9
3	estimate from GPS (Straub *et al.* 1997)		22 ± 3

It is difficult to estimate realistic errors in the velocities obtained from seismicity, given the uncertainty in the original M_s values. We consider it likely that the global M_s–M_0 relation yields an upper bound to the seismic moment release and that the regional relation yields a more realistic estimate. We may then conclude that the major portion (perhaps effectively all) of the motion in this region is probably achieved by seismic slip on faults, and that aseismic creep is relatively unimportant. However, this conclusion assumes that 500 years is long enough for a reasonable estimate of the long-term seismic moment rate, which, given periods of quiescence as long as 163 years (Table 1), may not be correct. In general, the smaller the region considered, the longer the sampling period needs to be for moment rates to be reliable (see e.g. Ambraseys & Jackson 1997).

5 CONCLUSIONS

The main conclusions from this study are as follows.

(1) The 20th century has been particularly active seismically in the Marmara region. Over the last 500 years only the 18th century has shown comparable activity, while periods with no earthquakes of $M_s \geq 6.8$ lasting 160 years are also known.

(2) Two regions of known late Quaternary faulting but with virtually no known significant earthquakes in the last 500 years stand out: the northwestern Sea of Marmara and the southern branch of the North Anatolian Fault east of Bursa. Prior to 1500, the strike-slip fault system east of Bursa is known to have been active, but this earlier period has revealed no substantial earthquakes from the northwestern Sea of Marmara.

(3) Historical earthquakes close to Istanbul have been offshore and with estimated magnitudes of M_s 6.8–7.2, smaller than those that have occurred east and west of the Sea of Marmara.

(4) It appears that the seismicity of the last 500 years can account for most of the expected 22 ± 3 mm yr^{-1} right-lateral slip in the Marmara region. Whether 500 years is long enough to obtain a reliable moment release rate is less clear.

ACKNOWLEDGMENTS

This is Cambridge Earth Sciences contribution ES 5907.

REFERENCES

Ambraseys, N.N., 1970. Some characteristic features of the North Anatolian fault zone, *Tectonophysics,* **9,** 143–165.

Ambraseys, N.N., 1988. Engineering seismology, *J. Earthq. Eng. Struct. Dyn.,* **17,** 1–105.

Ambraseys, N.N., 1992. Soil mechanics and engineering seismology, *Proc. 2nd National Conference on Geotechnical Engineering (invited paper),* Thessaloniki.

Ambraseys, N.N. & Finkel, C., 1987. The Saros-Marmara earthquake of 9 August 1912, *J. Earthq. Eng. Struct. Dyn.,* **15,** 189–211.

Ambraseys, N.N. & Finkel, C., 1995. *The Seismicity of Turkey and Adjacent Areas 1500-1800,* Eren publishers, Istanbul.

Ambraseys, N.N. & Jackson, J.A., 1997. Seismicity and strain in the Gulf of Corinth (Greece) since 1694, *J. Earthq. Eng.,* **1,** 433–474.

Ambraseys, N.N. & Jackson, J.A, 1998. Faulting associated with historical and recent earthquakes in the eastern Mediterranean region, *Geophys. J. Int.,* **133,** 390–406.

Ambraseys, N.N. & Sarma, S., 1999. The assessment of total seismic moment, *J. Earthq. Eng.,* **3,** 439–461.

Barka, A., 1996. Slip distribution along the North Anatolian Fault associated with the large earthquakes of the period 1939 to 1967, *Bull. seism. Soc. Am.,* **86,** 1238–1254.

Barka, A., 1999. The 17 August 1999 Izmit earthquake, *Science,* **285,** 1858–1859.

Barka, A. & Kadinsky-Cade, K., 1988, Strike-slip fault geometry in Turkey and its influence on earthquake activity, *Tectonics,* **7,** 663–684.

Ekström, G. & Dziewonski, A., 1988., Evidence of bias in estimation of earthquake size, *Nature,* **332,** 319–323.

Engdahl, E.R., van der Hilst, R. & Buland, R., 1998. Global teleseismic earthquake relocation with improved travel times and procedures for depth determination. *Bull. seism. Soc. Am.,* **88,** 722–743.

McClusky, S. *et al.*, 2000. GPS constraints on plate motions and deformations in the Eastern Mediterranean: implications for plate dynamics, *J. geophys. Res.,* in press.

McKenzie, D., 1978. Active tectonics of the Alpine-Himalayan belt: the Aegean Sea and surrounding regions, *Geophys. J. R. astr. Soc.,* **55,** 217–254.

Okay, A.I., Demirbag, E., Kurt, H., Okay, N. & Kuscu, I., 1999. An active, deep marine strike-slip basin along the North Anatolian Fault, Turkey, *Tectonics,* **18,** 129–147.

Papazachos, C.B., 1992. Anisotropic radiation modelling of macroseismic intensities for estimation of the attenuation structure of the upper crust in Greece, *Pure appl. Geophys.,* **138,** 445–469.

Parke, J.R. *et al.*, 2000. Active faults in the Sea of Marmara, western Turkey, imaged by seismic reflection profiles, *Terra Nova,* in press.

Scholz, C.H., Aviles, C. & Wesnousky, S., 1986. Scaling differences between large intraplate and interplate earthquakes, *Bull. seism. Soc. Am.,* **76,** 65–70.

Smith, A.D., Oktay, F., Taymaz, T., Jackson, J., Basaran, H., Alpar, B., Simsek, M. & Kara, S., 1995. High resolution seismic profiling in the Sea of Marmara (NW Turkey): Late Quaternary sedimentation and sea-level changes, *Geol. Soc. Am. Bull.,* **107,** 923–936.

Stein, R., Barka, A. & Dietrich, J., 1997. Progressive earthquake failure on the North Anatolian Fault since 1939 by stress triggering, *Geophys. J. Int.,* **128,** 594–604.

Straub, C., Kahle, H.-G. & Schindler, C., 1997. GPS and geologic estimates of the tectonic activity in the Marmara Sea region, NW Anatolia, *J. geophys. Res.,* **102,** 27 587–27 601.

Taymaz, T., Jackson, J. & McKenzie, D., 1991. Active tectonics of the north and central Aegean Sea, *Geophys. J. Int.,* **106,** 433–490.

Toksöz, M.N., Reilinger, R.E., Doll, C.G., Barka, A.A. & Yalcin, N., 1999. Izmit (Turkey) earthquake of 17 August 1999: first report, *Seism. Res. Lett.,* **70,** 669–679.